

# Scintillation measurements at Bahir Dar during the high solar activity phase of solar cycle 24

Norbert Jakowski<sup>1</sup>, Martin Kriegel<sup>1</sup>, Hiroatsu Sato<sup>1</sup>, Jens Berdermann<sup>1</sup>, Volker Wilken<sup>1</sup>, Stefan Gewies<sup>1</sup>, Nikolai Hlubek<sup>2</sup>, Mogese Wassae<sup>3</sup>, and Baylie Damtie<sup>3</sup>

<sup>1</sup> Institute of Communications and Navigation, German Aerospace Center, Neustrelitz, Germany

<sup>2</sup> gateprotect GmbH, Leipzig, Germany

<sup>3</sup> Washera Geospace and Radar Science Laboratory, Bahir Dar University, Ethiopia

A large, curved image of the Earth from space occupies the bottom half of the slide. It shows a portion of the African continent, the Middle East, and parts of Europe and Asia, with blue oceans and green landmasses. The Earth's atmosphere is visible as a thin blue layer at the top of the curve.

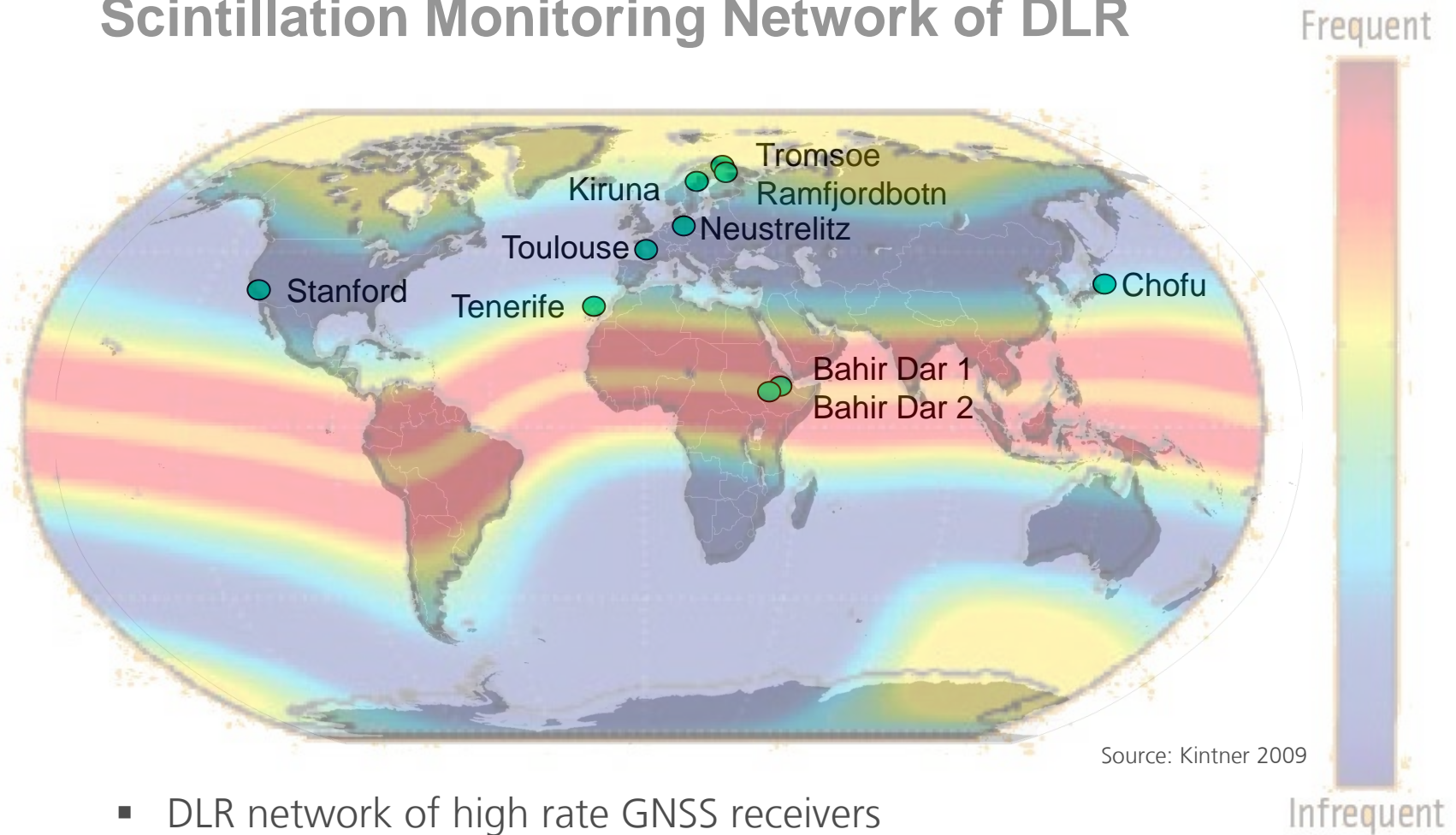
Knowledge for Tomorrow

# Outline

- Introduction
- Data base and monitoring techniques
- Data analysis
- Observations
- Preliminary two-station case study
- Summary & Conclusions



# Scintillation Monitoring Network of DLR



- DLR network of high rate GNSS receivers
- Network provides scintillation data distributed via IMPC/SWACI  
<http://swaciweb.dlr.de>





# Current scintillation receiver network in Bahir Dar



Javad receiver,  
50 Hz sampling  
rate



● DLR 1

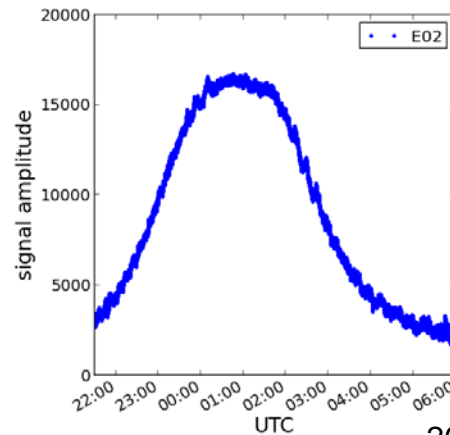
● Sites with receiver



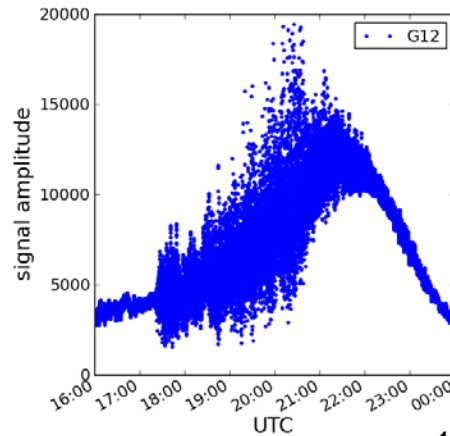
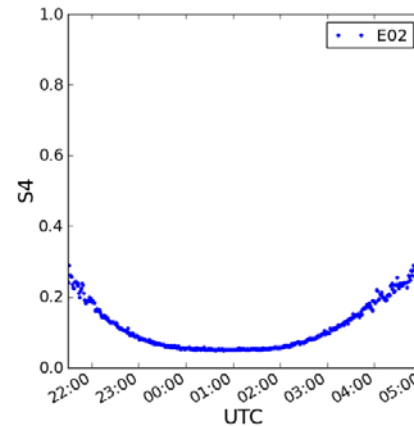
Installation of DLR GNSS 2  
in June 2014



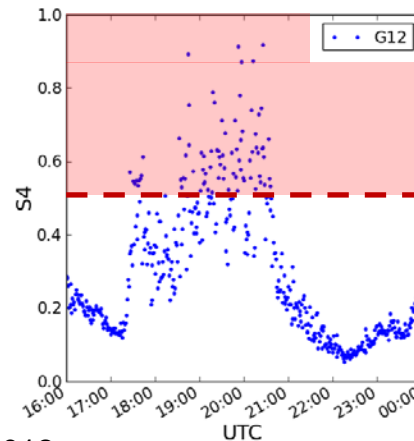
# Amplitude scintillations



26-27/01/2012



10-11/04/2012



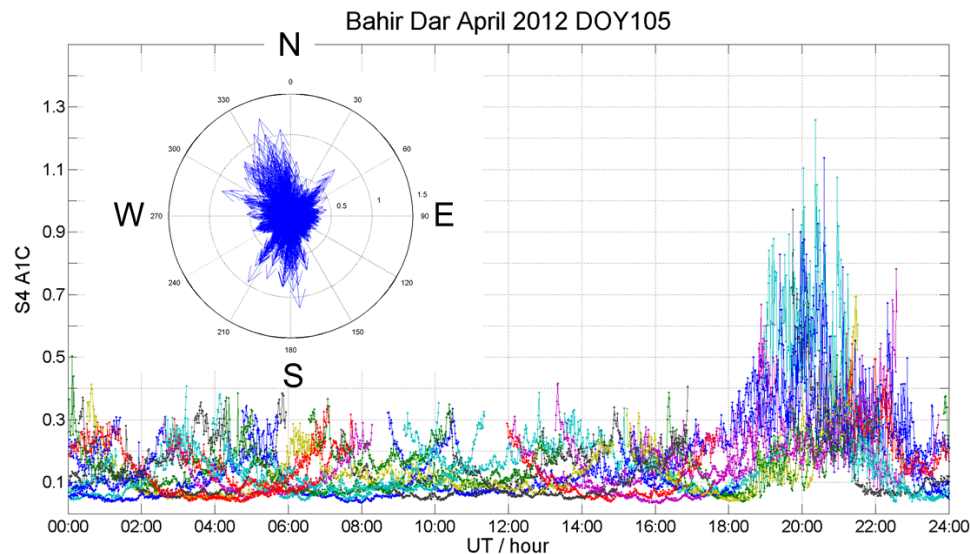
$$S_4 = \left( \frac{\langle SI^2 \rangle - \langle SI \rangle^2}{\langle SI \rangle^2} \right)^{1/2}$$

Enhancement of  $S_4$  at low elevation due to multipath effects. Effect has to be mitigated in subsequent analysis.

$S_4$	
< 0.3	low noise
0.3 to 0.5	enhanced
> 0.5	scintillation event

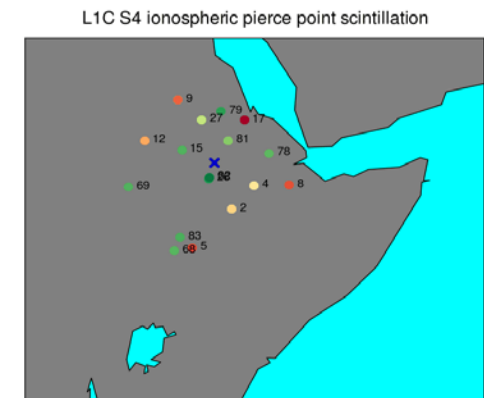
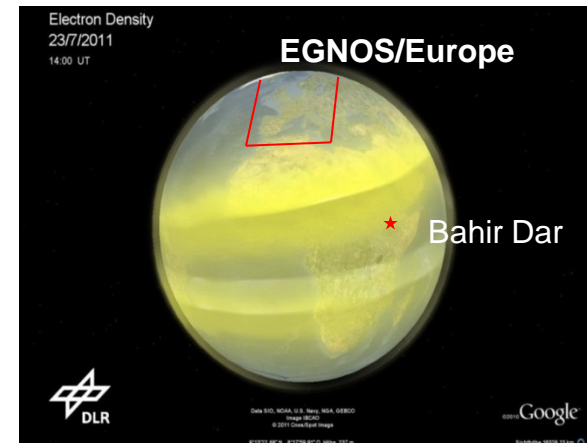


# Diurnal variation of scintillation activity at Bahir Dar

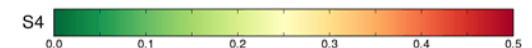


$S_4$  Scintillation activity enhances regularly in Bahir Dar / Ethiopia after sunset

Scintillations occur primarily in North-South direction

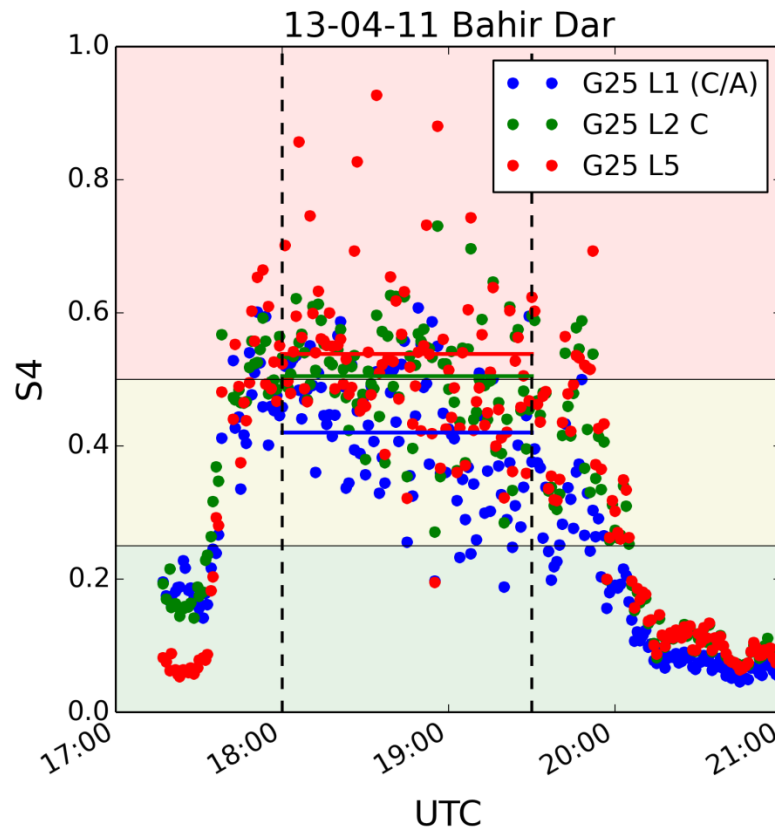


Time: 2012-04-10 17:00





## Different GNSS signals - one day one satellite



Signal	Mean	Std. dev.
L1 (C/A)	0.42	0.098
L1 p(y)	0.64	0.11
L2 p(y)	0.63	0.11
L2 C	0.50	0.084
L5	0.54	0.183

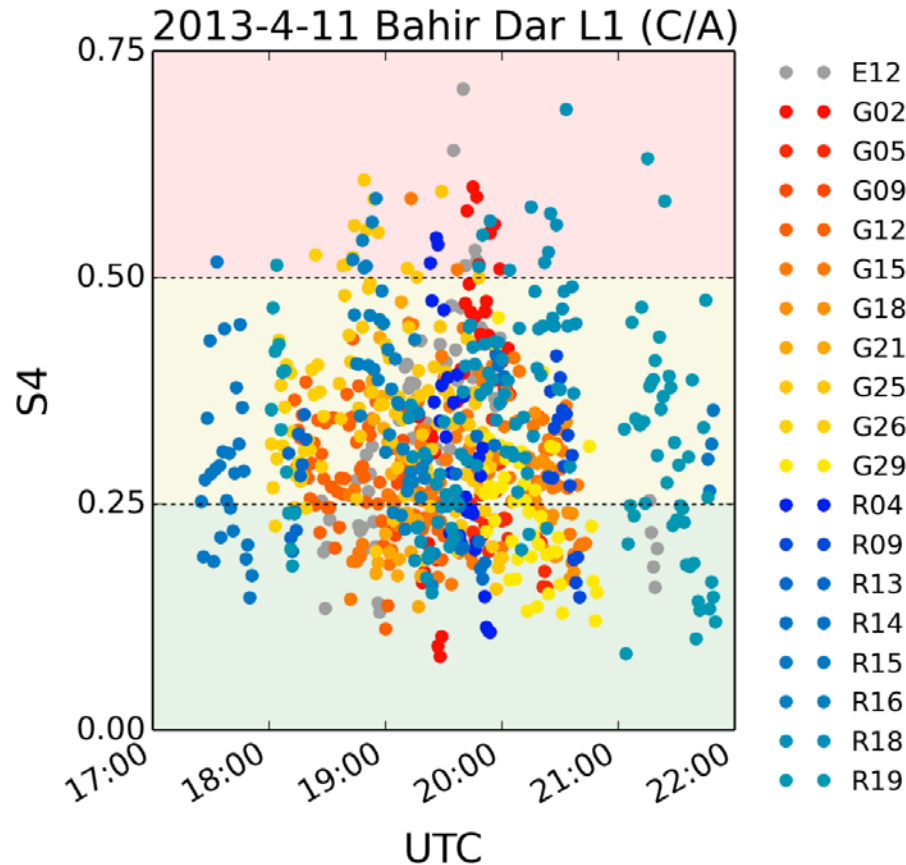
Precise p-code could not be encrypted,  
reconstruction technology degrades SNR.

Encrypted signals are ignored in  
subsequent analysis.

[Hlubek et al. , SWSC, 4, A22, 2014]



# Preprocessing of scintillation events



Problem:

Only few large events with  $S_4 > 0.5$ , not sufficient for statistical analysis

Solution:

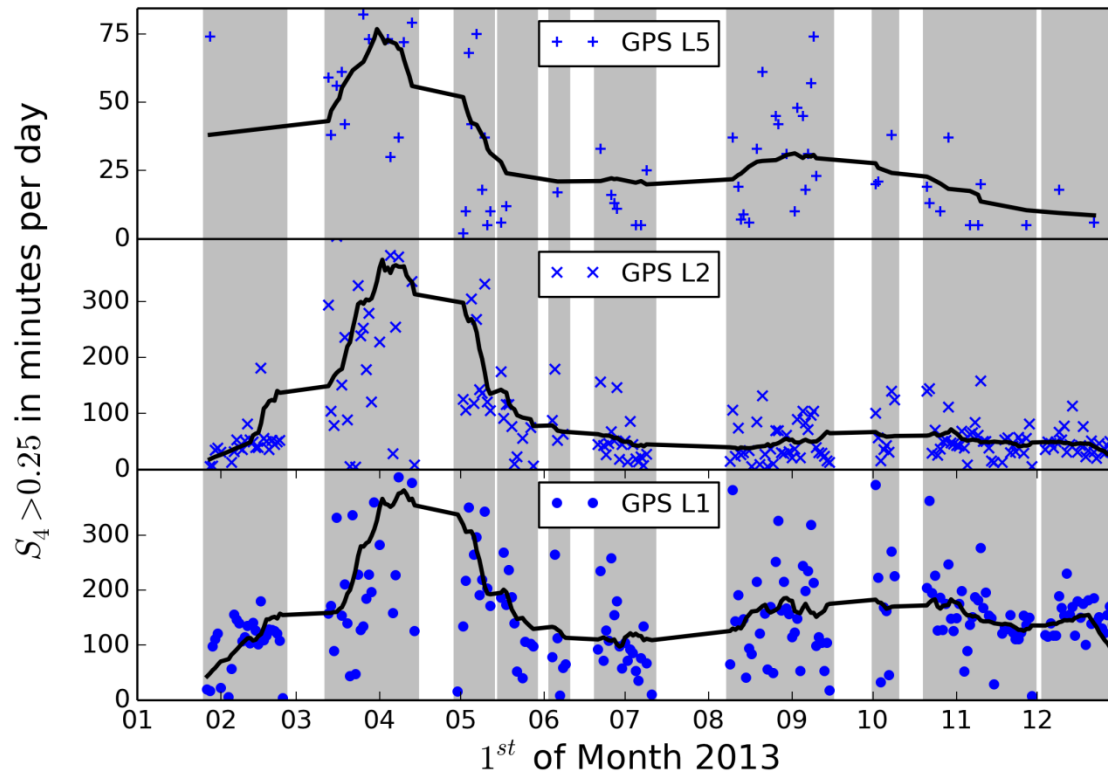
Elimination of weak scintillation events whose origin is unknown with soft barrier around  $S_4=0.25$

[Hlubek et al. , SWSC, 4, A22, 2014]





# Seasonal variation of scintillation occurrence - GPS



Occurrence peaks at equinoxes

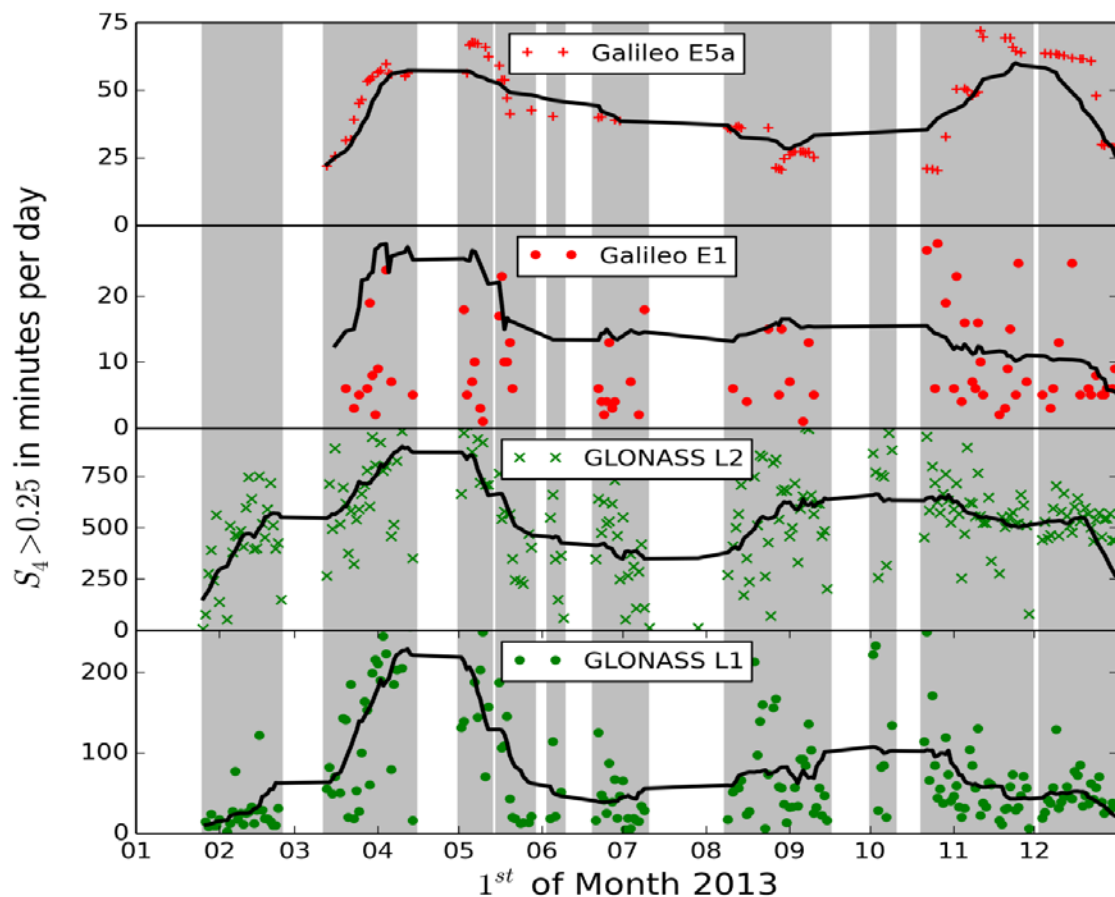
Significant difference between spring and autumn equinoxes, probably due to different levels of solar activity:

Spring :  $\langle R_z \rangle = 57.1$

Autumn:  $\langle R_z \rangle = 44.0$



## Seasonal variation of scintillation occurrence – GLONASS, Galileo



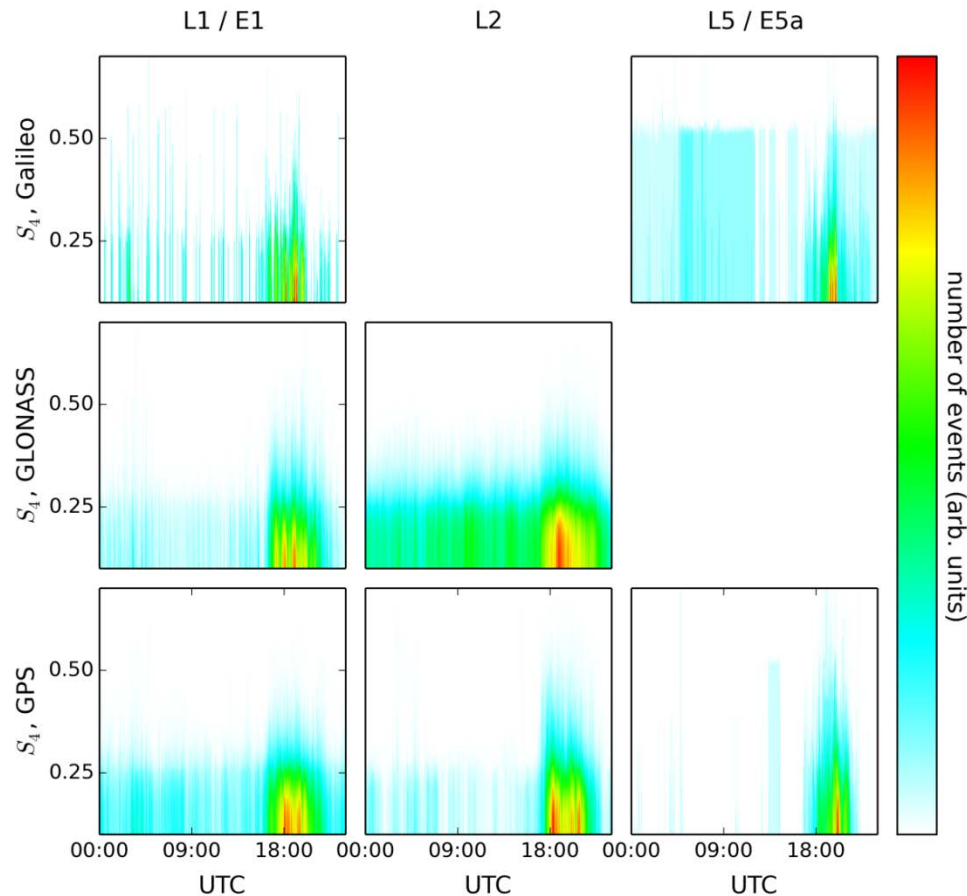
Occurrence peaks at equinoxes

Significant difference between spring and autumn equinoxes, probably due to different levels of solar activity:  
 Spring :  $\langle R_z \rangle = 57.1$   
 Autumn:  $\langle R_z \rangle = 44.0$

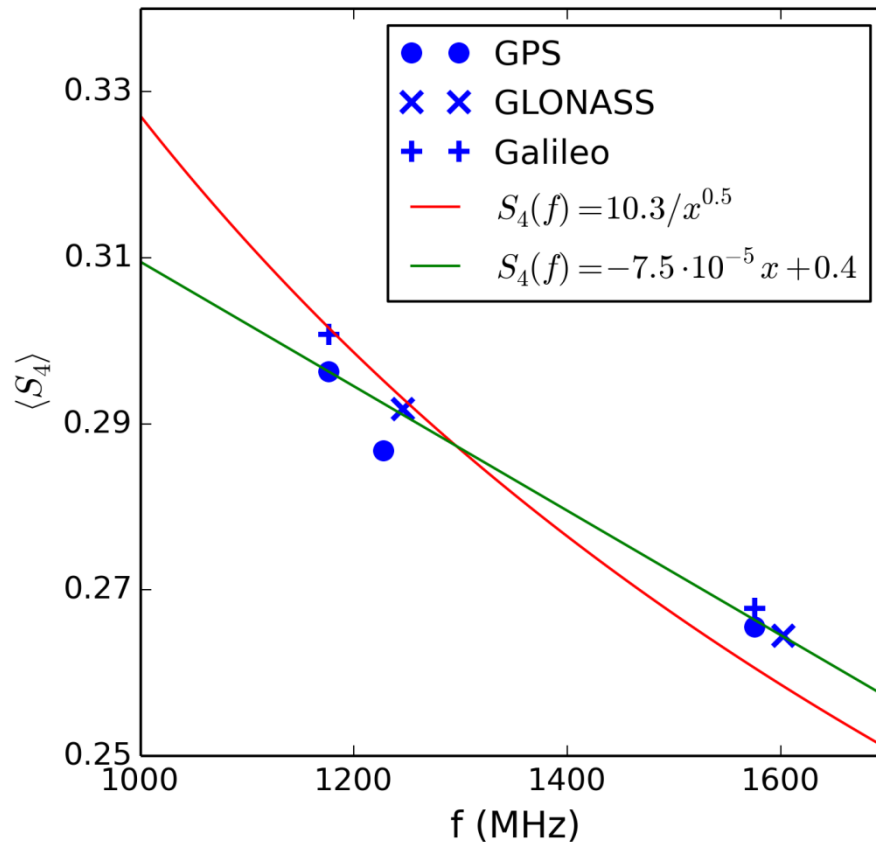
All GNSS show similar behavior at mostly all frequencies.



## Diurnal variation of scintillation occurrence



# Scintillation strength as function of frequency



Observed frequency dependence covers only a small frequency range.

Ogawa et al. (1980)  
found for  $136 \leq f \leq 1700$  MHz:

$$S_4 \sim 1 / f^{0.5}$$

agrees with L1-L2-L5 tendency

[Ogawa et al. , JATP, 42(7),1980]



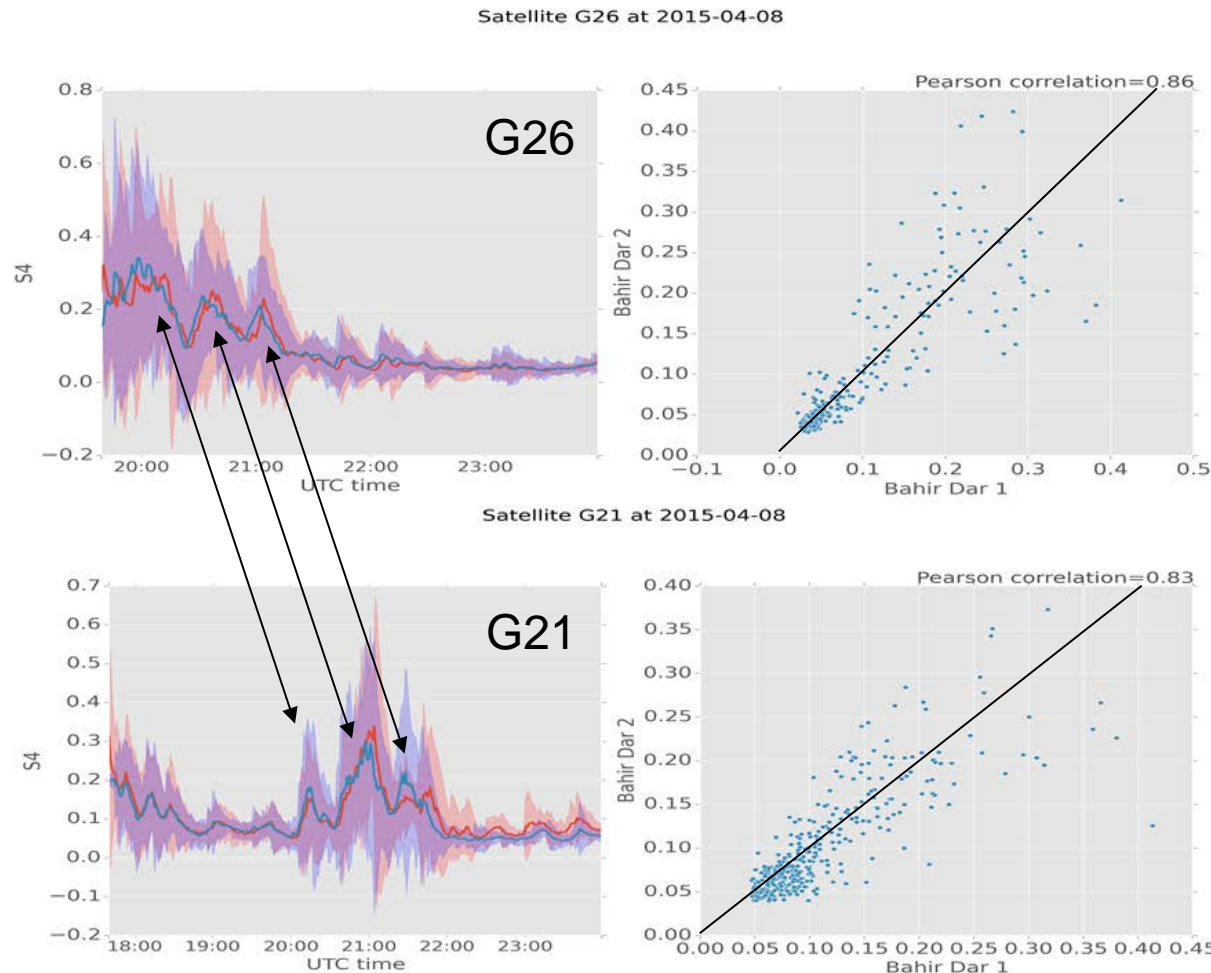


# Outline

- Introduction
- Data base and monitoring techniques
- Data analysis
- Observations
- Preliminary two-station case study
- Summary & Conclusions



# S<sub>4</sub> correlation of both DLR stations on 8 April 2015



Distance: 7.16 km

Direction:  
 $\approx$  East (I) – West (II)

Left panel  
 Mean S<sub>4</sub> index  
 Background:  $\pm 4 \sigma$   
 Station I: red  
 Station II: blue

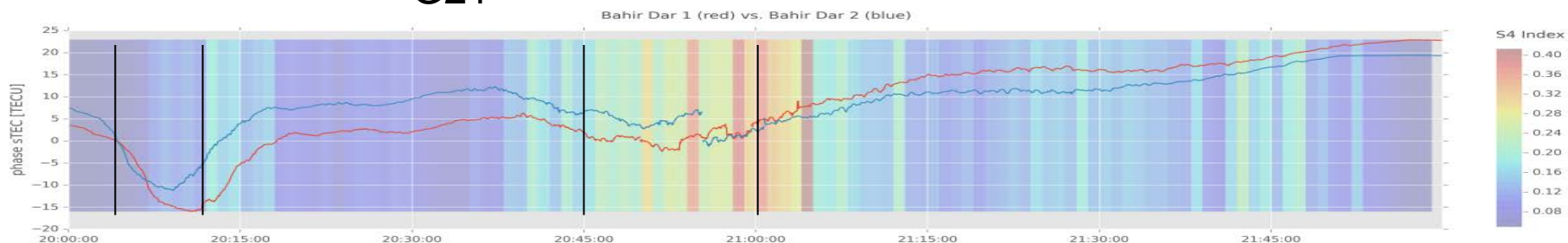
Right panel  
 Cross correlation of  
 S<sub>4</sub> from both stations



# TEC depletions on 8 April 2015

G21

Satellite G21 at 2015-04-08



TEC depletion I

$\Delta \text{STEC}_I \approx 18 \text{ TECU}$

$T_{\text{Dep}} \approx 7.5 \text{ min}$

$S_{4\text{max}} \approx 0.2$

TEC depletion II

$\Delta \text{STEC}_{II} \approx 9 \text{ TECU}$

$T_{\text{Dep}} \approx 15 \text{ min}$

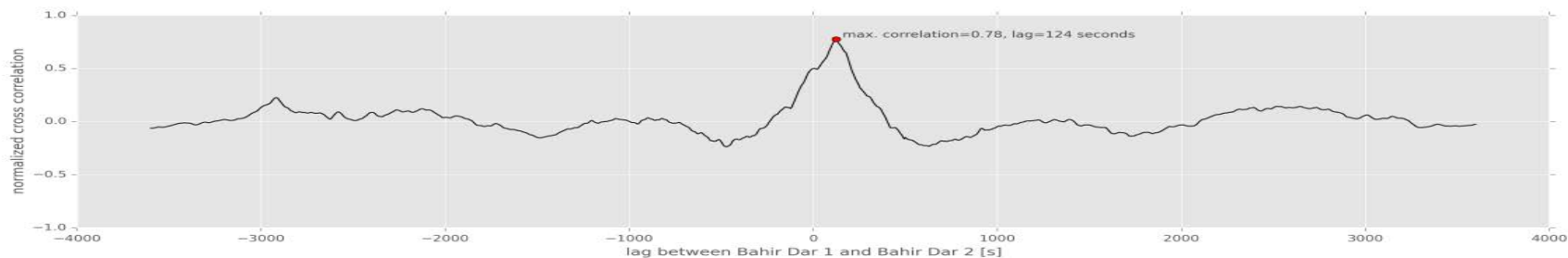
$S_{4\text{max}} \approx 0.4$

East-west distance between

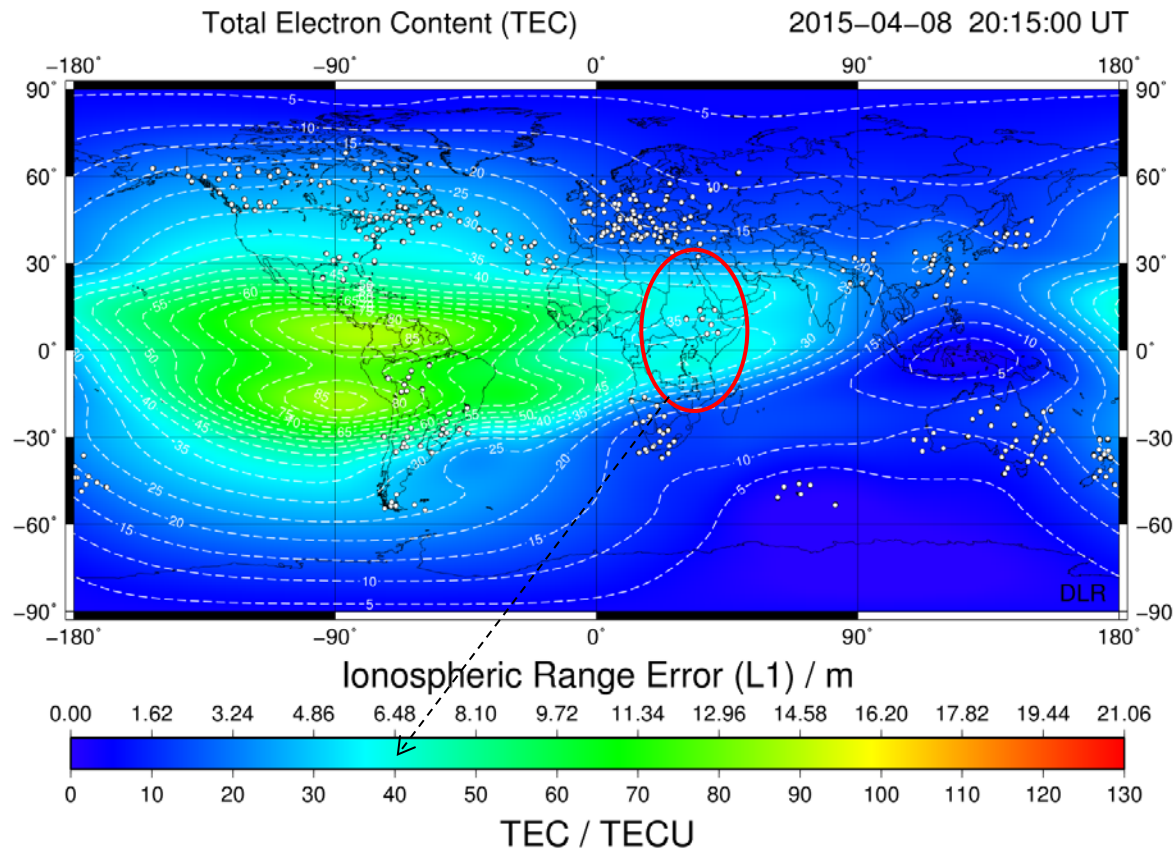
stations: 7.16 km

Time delay: 124 s

Max(cc): 0.78



# Background ionization provided by TEC



Global TEC mapping in near real time is based on 1 s GNSS data from geodetic networks (ASI, IGS, EUREF) provided in streaming mode via NTRIP technology.

Actual data products incl. [movies](#) available via DLR IMPC service.

<http://swaciweb.dlr.de>

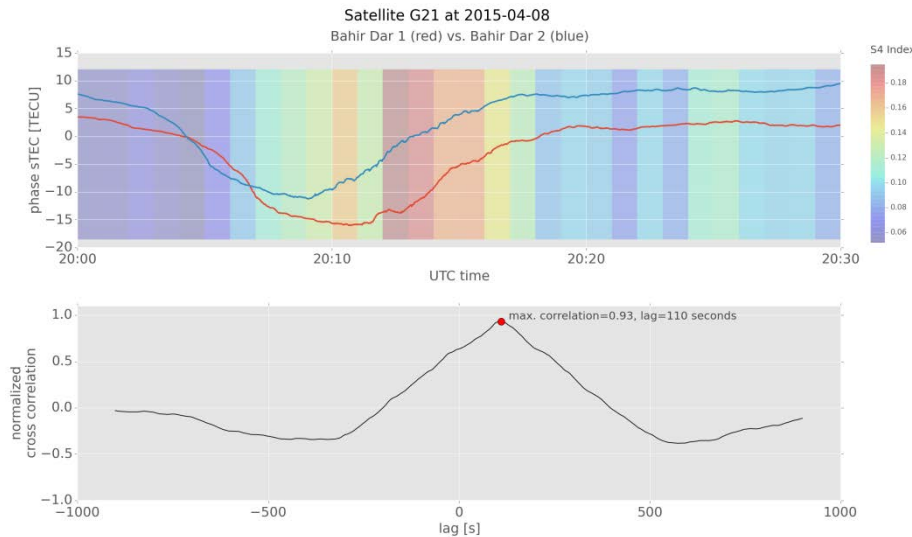
$$\Delta\text{TEC}_{-(I,II)} \approx 20 - 30\%$$

Background model: Jakowski et al, J. Geod., 85(12), 965–974, 2011  
Mapping technique: Jakowski et al., Radio Sci., 46, RS0D18, 2011





# TEC depletion around 20:10 UT at G21/26

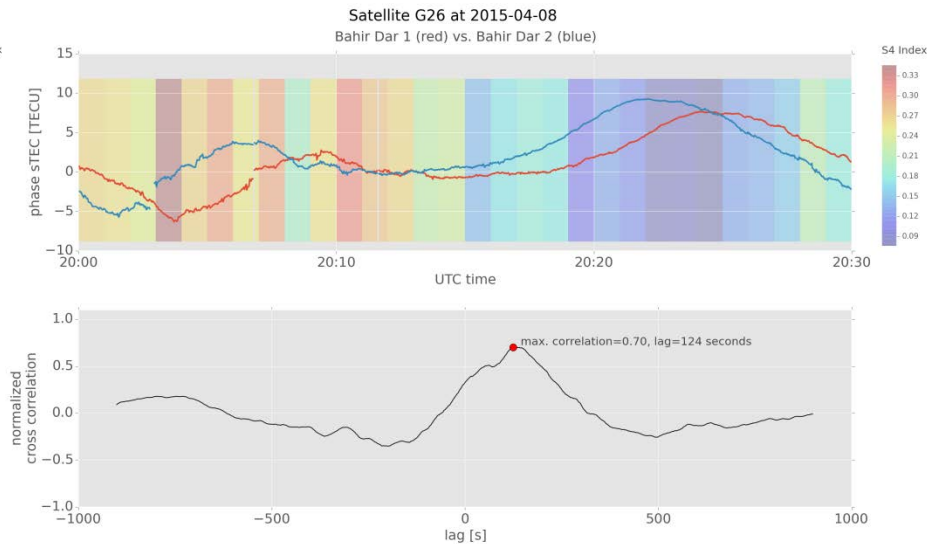


TEC depletion 1/G21

Max(cc): 0.93

lag: 110 s

$v_O \approx 65$  m/s ( $v_D \approx 80$  m/s)



TEC depletion 1/G26

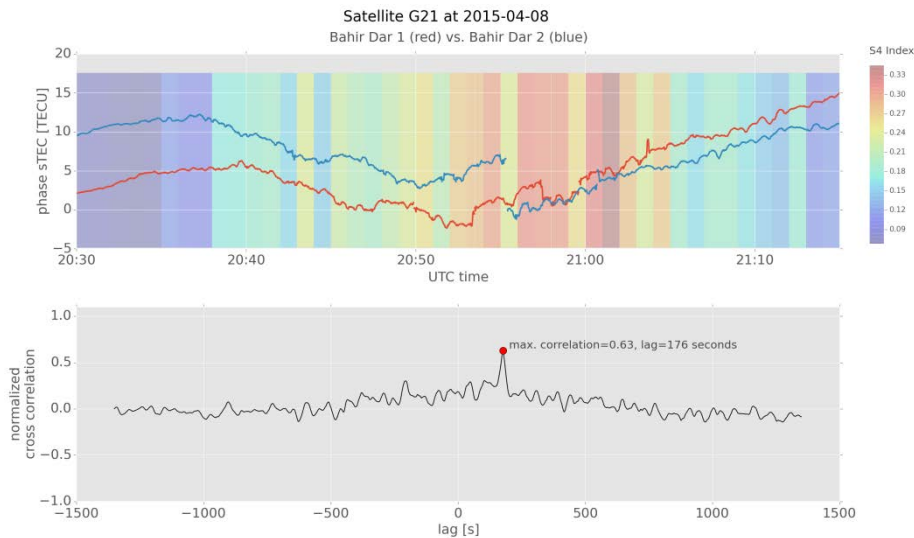
Max(cc): 0.70

lag: 124 s

$v_O \approx 58$  m/s ( $v_D \approx 84$  m/s)



# TEC depletion around 20:50 UT at G21/26

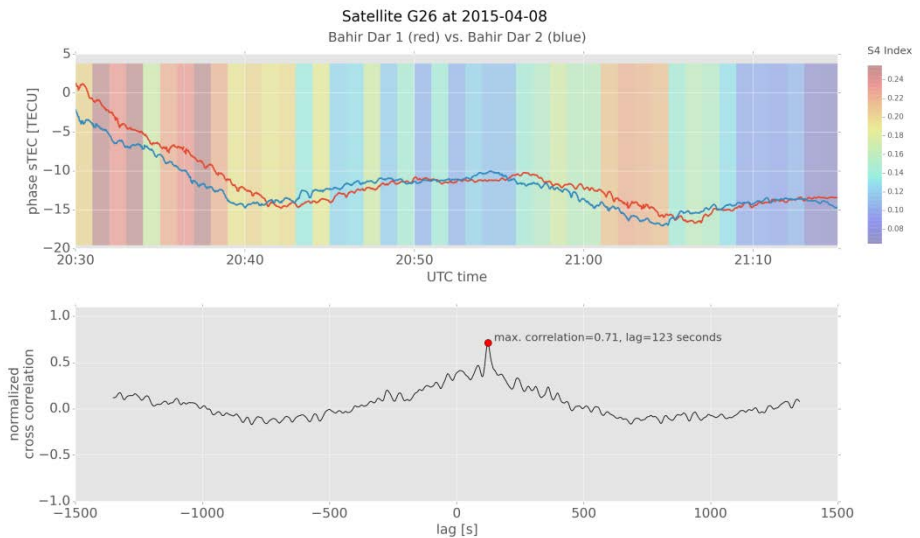


TEC depletion 2/G21

Max(cc): 0.63

lag: 176 s

$v_O \approx 41 \text{ m/s}$  ( $v_D \approx ? \text{ m/s}$ )



TEC depletion 2/G26

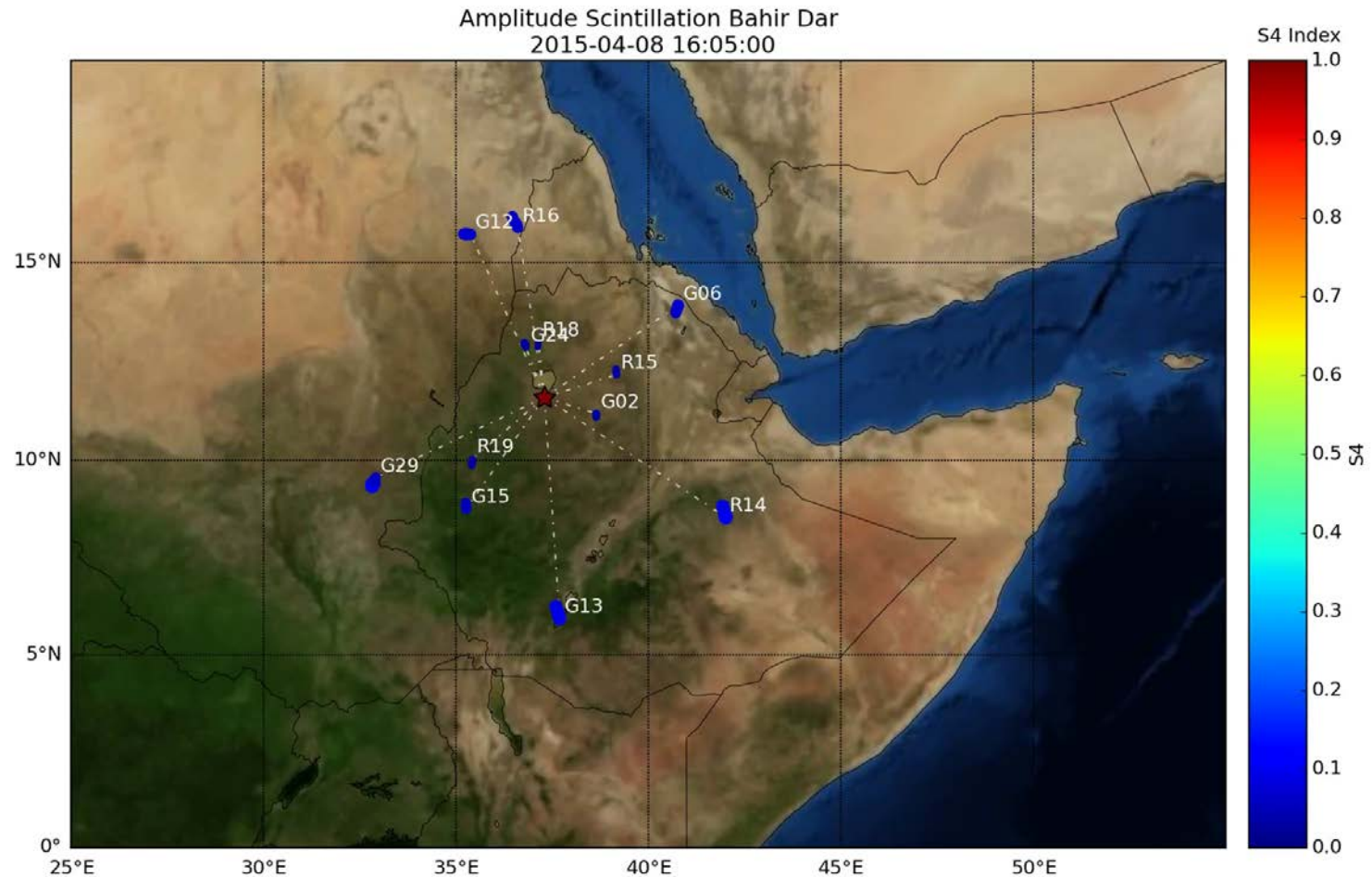
Max(cc): 0.71

lag: 123 s

$v_O \approx 58 \text{ m/s}$  ( $v_D \approx 78 \text{ m/s}$ )

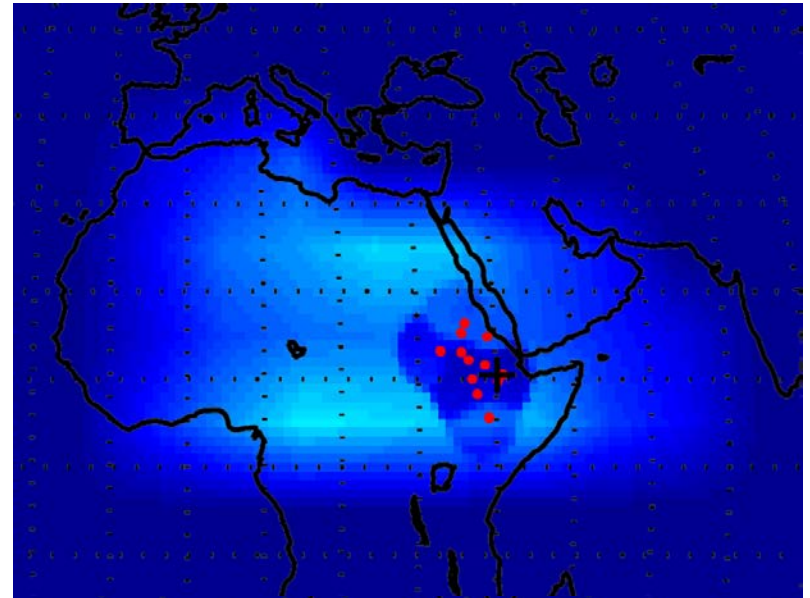
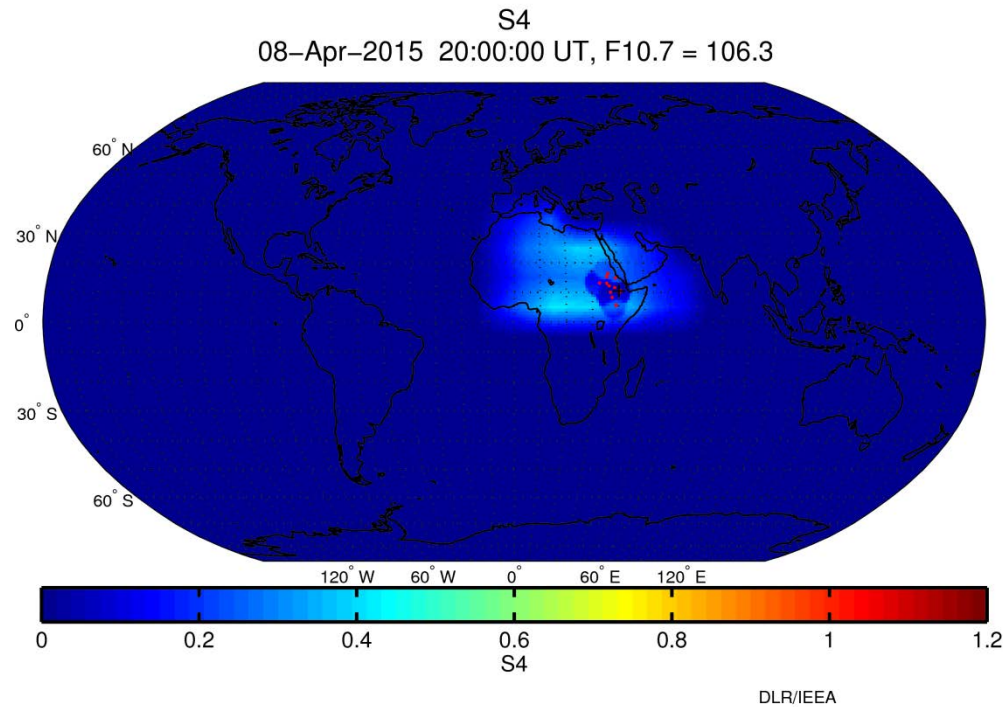


# Scintillation activity along different satellite links





# Scintillation map on 8 April, 2015, 20:00 UT

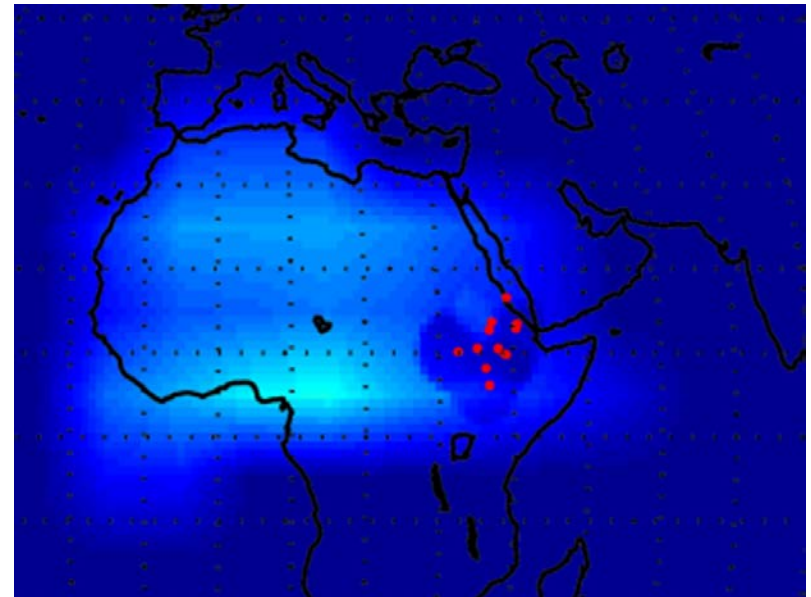
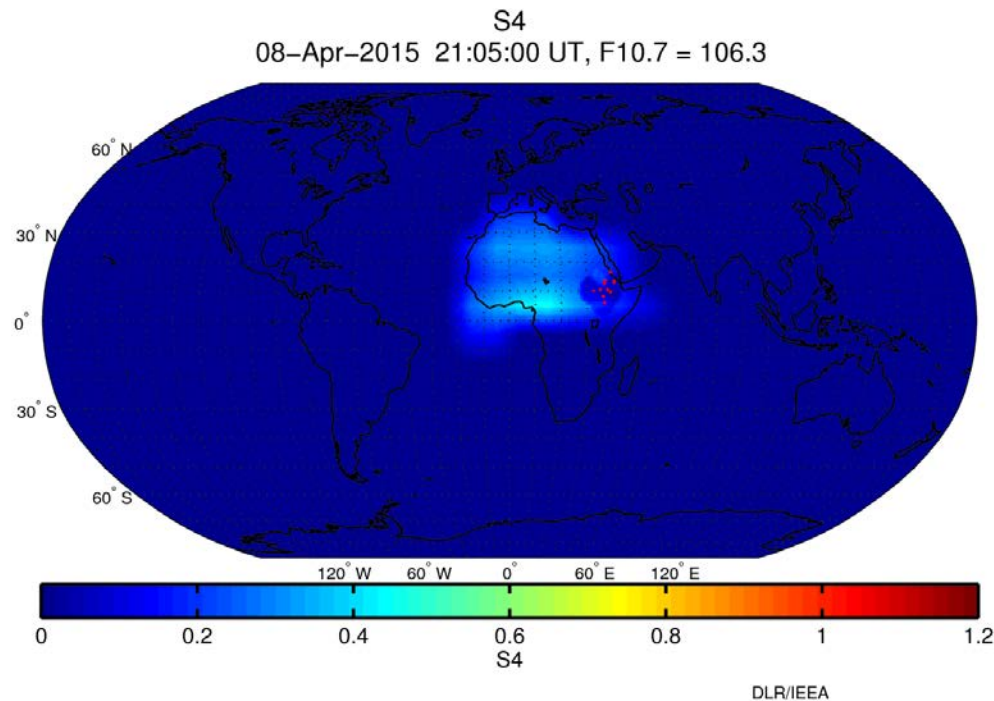


GISM model: Beniguel & Hamel, SWSC, 2011  
Mapping technique: Jakowski et al., Radio Sci., 2011





# Scintillation map on 8 April, 2015, 21:05 UT



GISM model: Beniguel & Hamel, SWSC, 2011  
Mapping technique: Jakowski et al., Radio Sci., 2011



## Summary & conclusion

- Seasonal statistics of  $S_4$  with maxima around equinoxes confirms former studies, asymmetry between spring and autumn needs further investigation.
- GPS, GLONASS and Galileo systems show different sensitivity to ionospheric irregularities.
- Local network of scintillation receivers in Bahir Dar allows detecting plasma bubbles and their drift velocities.
- Availability of different GNSS makes scintillation mapping attractive.
- To explore the structure and dynamics of plasma bubbles, the current local GNSS network should be extended.
- Comparative measurements with complementary techniques should be performed.



# Thank you for your attention!

Contact:

Dr. Norbert Jakowski  
Kalkhorstweg 53  
D-17235 Neustrelitz  
Germany

Tel. +49 (0)3981 480 - 151

Fax. +49 (0)3981 480 - 123

Email: [Norbert.Jakowski@dlr.de](mailto:Norbert.Jakowski@dlr.de)

Web: [www.dlr.de/kn](http://www.dlr.de/kn) <http://swaciweb.dlr.de>